Electronic Supplementary Material (ESI) for Sustainable Energy & Fuels.

Unravelling the Chemistry of Catalyst Surface and Solvent towards C-C Bond Formation through Activation and Electrochemical Conversion of CO_2 into Hydrocarbons over Micro-structured Dendritic Copper

Nusrat Rashid[1], Mohsin Ahmad Bhat[2], Pravin P. Ingole[1*]

[1]Department of Chemistry, Indian Institute of Technology Delhi, New Delhi, India 110016.

[2]Department of Chemistry, University of Kashmir, Srinagar, Jammu and Kashmir, India

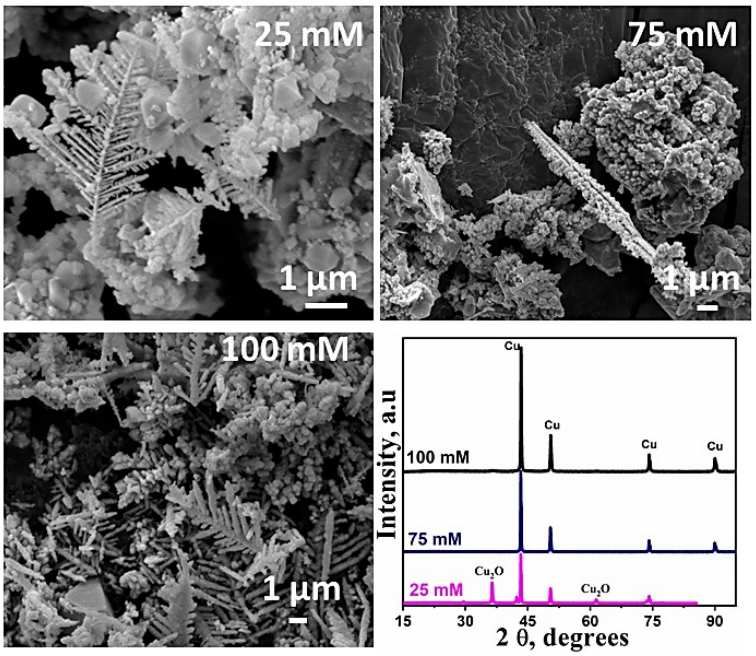

Figure SI-1: The representative SEM images and XRD patterns of the Cu-microstructures prepared at varying AsH concentration used during the electrodepostion process.

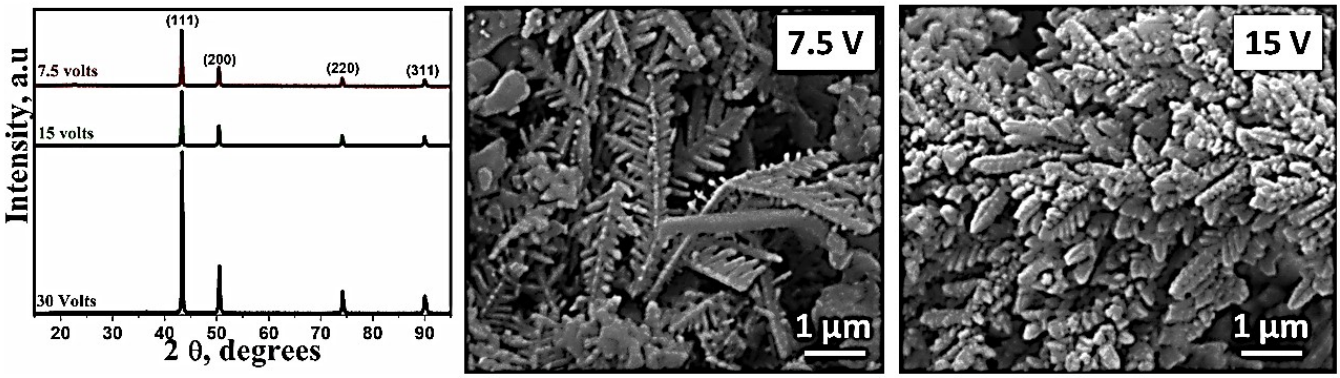

Figure SI-2: The representative XRD patterns and SEM images of the Cu-microstructures prepared at varying biases applied during the electrodepostion process. The SEM image for 30 V sample is not shown as it is the same sample obtained with 100 mM AsH concentration shown in Figure SI-2.

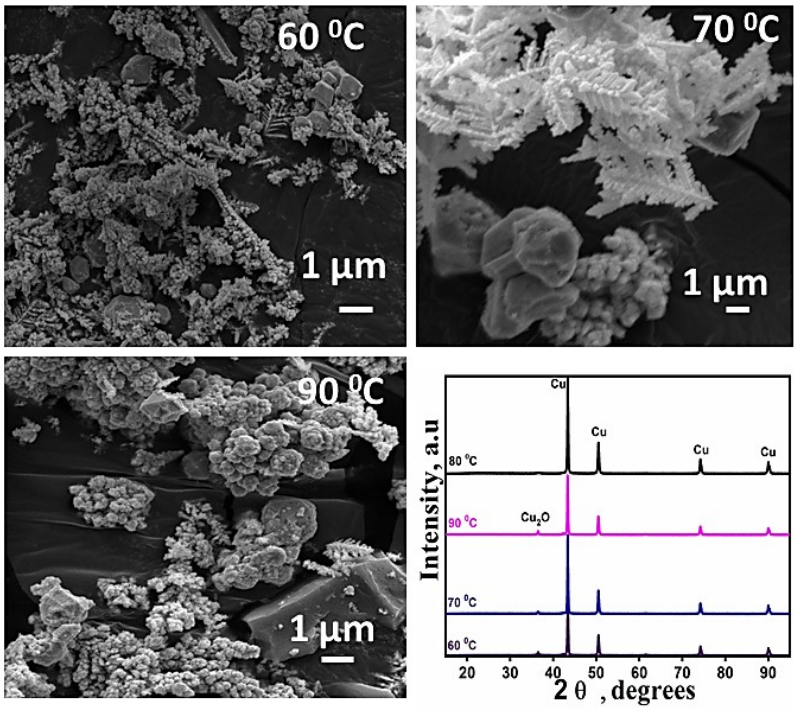

Figure SI-3: SEM images and XRD patterns of the Cu-microstructures prepared at varying electrodepostion bath temperatures. The SEM image for 80 ^{0}C sample is not shown as it is the same sample obtained with 30 V bias and 100 mM AsH concentration shown in Figure SI-2.

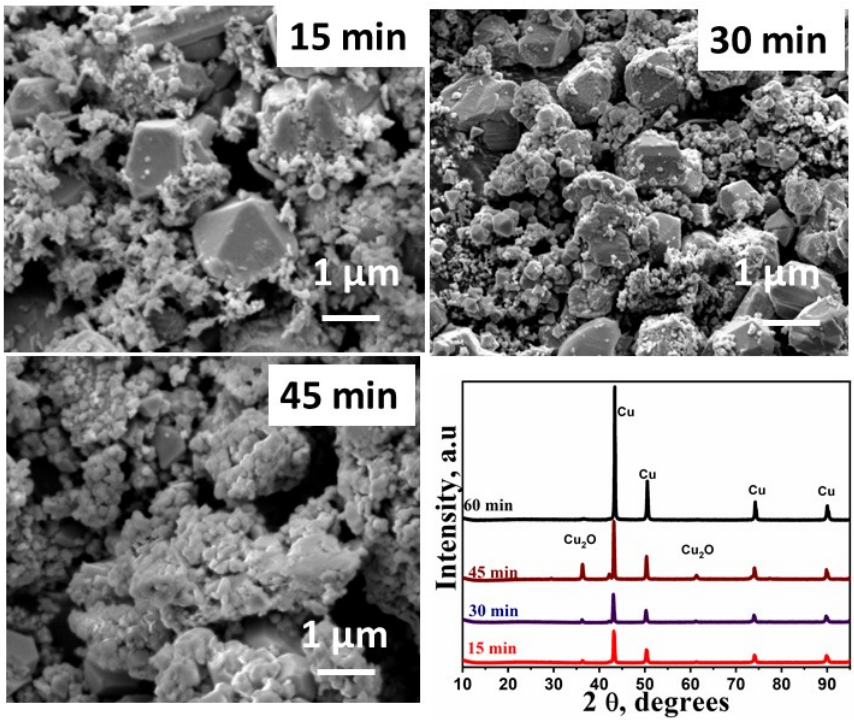

Figure SI-4: SEM images and XRD patterns of the Cu-microstructures prepared at varying electrodepostion times. The SEM image for 60 minutes sample is not shown as it is the same sample obtained with 60 ^{o}C, 30 V bias and 100 mM AsH concentration shown in Figure SI-2.

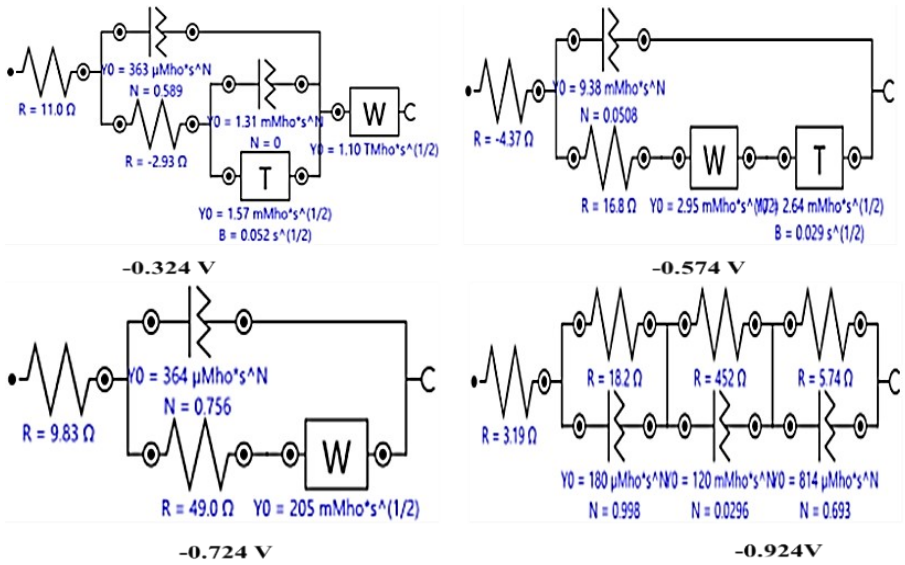

Figure SI-5: An equivalent circuits fitted to the Nyquist plots obtained on the most active Cu-micrstructures in CO_2 saturated 0.2 M $KHCO_3$ at different potentioals.

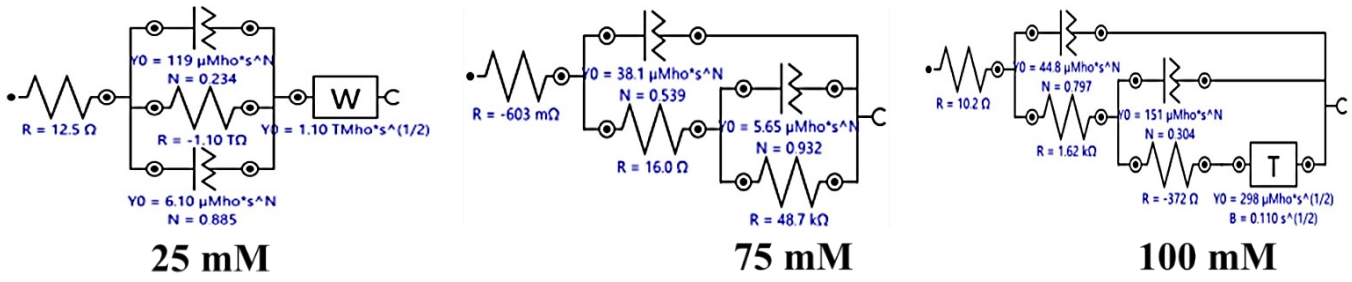

Figure SI-6: An equivalent circuits fitted to the Nyquist plots obtained on different Cu-micrstructures in CO_2 saturated 0.2 M $KHCO_3$ at OCP. Due to different microstructure these catalysts behave differently, suggesting role of nano-morphology in charge transfer dynamics.

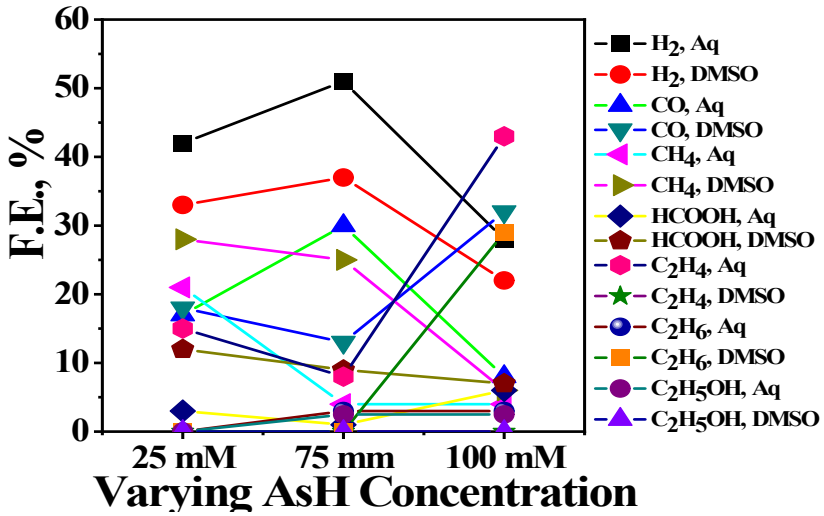

Figure SI-7. A comparison of the trend in variation of F.E. values for Cu-microstructure catalysts (prepared with varying concentrations of AsH) in DMSO and $KHCO_3$ aqueous medium.

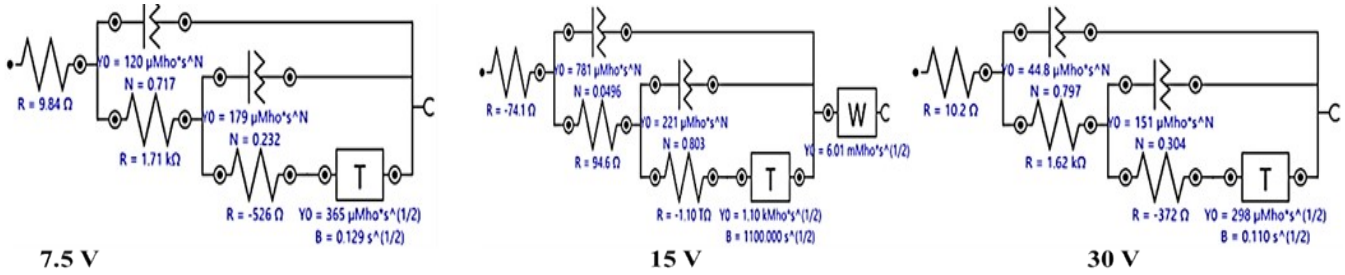

Figure SI-8: An equivalent circuits fitted to the Nyquist plots obtained on different Cu-microstructures in CO_2 saturated 0.2 M $KHCO_3$ at OCP. Due to similarity in microstructure shapes i.e. dendrimeric at 30 V, or small dendritic clusters at 7.5 V and 15 V, these catalysts behave similarly, albiet differing in the values for charge tranfer dynamic parameters.

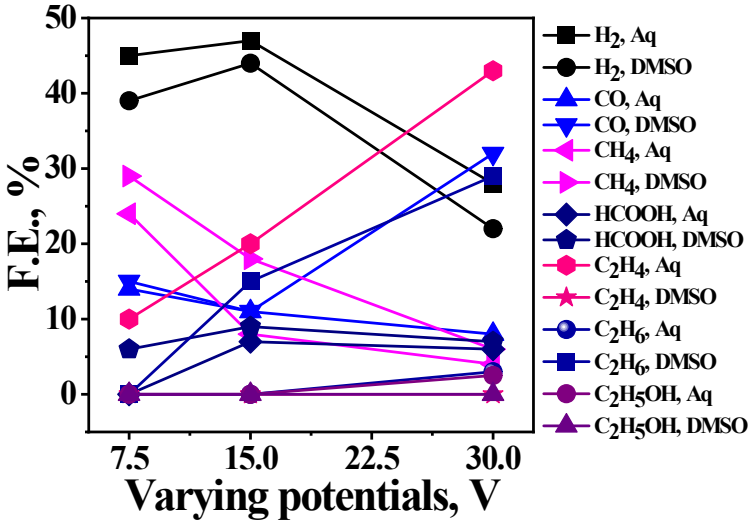

Figure SI-9. A comparison of the trend in variation of F.E. values for Cu-microstructure catalysts (prepared at varying applied bias) in DMSO and $KHCO_3$ aqueous medium.

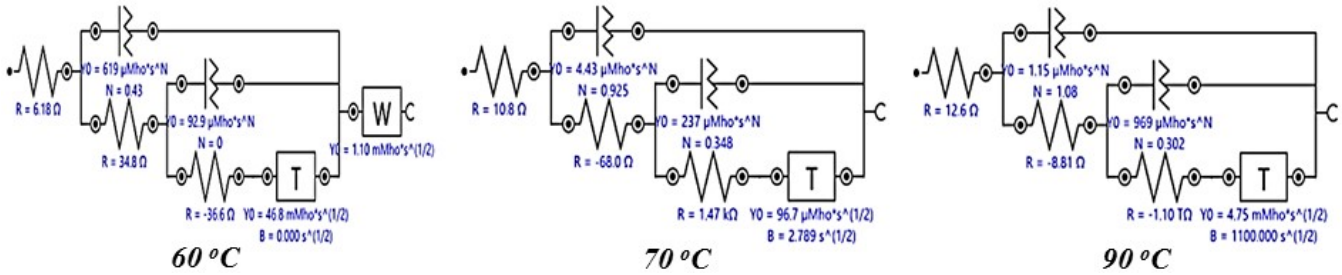

Figure SI-10: An equivalent circuits fitted to the Nyquist plots obtained on different Cu-micrstructures in CO_2 saturated 0.2 M $KHCO_3$ at OCP. Except for the additional warburg element in 60°C, the representative equivalent circuits for other ctalysts have similar elements, reinforcing that similar nano-morphology behaves in similar ways albiet with different values for the elements constituting the circuit.

Table SI-1: Different products obtained at different surfaces in 0.2M $KHCO_3$ and DMSO in a CO_2-saturated solution at -1.0V (RHE) (NHE in DMSO). The table also shows the product selectivity dependence on the applied potential at 60 min catalyst (optimized dendritic structure).

Samples	H_2	CO	CH_4	HCOOH	F.E. for C1	C_2H_4	C_2H_6	C_2H_5OH	F.E. for C2	C1 + C2	Total	Selectivity (in %) For C1	Selectivity (in %) for C2
25 mM	42	17	21	3	24	15	0	0	15	39	98	61.5	38.5
DMSO	33	18	28	12	40	0	0	0	0	40	91	100	0
75 mM	51	30	4	1	5	8	3	2.5	13.5	18.5	99.5	27	73
DMSO	37	13	25	9	34	0	0	0	0	34	84	100	0
100 mM	28	8	4	6	10	43	3	2.5	48.5	58.5	94.5	17	83
DMSO	22	32	6	7	13	0	29	0	29	42	96	31	69
7.5 V	45	14	24	0	24	10	0	0	10	34	93	71	29
DMSO	39	15	29	6	35	0	0	0	0	35	89	100	0
15 V	47	11	8	7	15	20	0	0	20	35	93	43	57
DMSO	44	11	18	9	27	0	15	0	15	42	97	64	36
30 V	28	8	4	6	10	43	3	2.5	48.5	58.5	94.5	17	83
DMSO	22	32	6	7	13	0	29	0	29	42	96	31	69
60	44	12	28	0	28	12	0	4	16	44	100	63	37
DMSO	51	16	22	8	30	0	0	0	0	30	97	100	0
70	39	8	25	4	29	17	3	2.5	22.5	51.5	98.5	56	44
DMSO	44	17	25	3	28	0	0	0	0	28	89	100	0
80	28	8	4	6	10	43	3	2.5	48.5	58.5	94.5	17	83
DMSO	22	32	6	7	13	0	29	0	29	42	96	31	69
90	45	36	10	0	10	0	0	0	0	10	91	100	0
DMSO	55	17	28	0	28	0	0	0	0	28	100	100	0
15 min	37	49	0	5	5	0	0	0	0	5	91	100	0
DMSO	39	19	26	13	39	0	0	0	0	39	97	100	0
30 min	26	28	23	10	33	0	0	0	0	33	87	100	0
DMSO	31	17	24	19	43	0	0	0	0	43	91	100	0
45 min	35	20	15	2	17	12	3	2.5	17.5	34.5	89.5	49	51
DMSO	49	15	25	6	31	0	0	0	0	31	95	100	0
60 min	28	8	4	6	10	43	3	2.5	48.5	58.5	94.5	17	83
DMSO	22	32	6	7	13	0	29	0	29	42	96	31	69
	For 60 min in 0.2 M $KHCO_3$ at different applied potentials.												
-0.32 V	28	41	3	0	3	0	0	0	0	3	72	100	0
-0.57 V	36	49	8	2	10	3	0	0	3	13	98	77	23
-0.72 V	41	21	17	0	17	12.5	0	0	12.5	29.5	91.5	58	42
-0.92 V	37	22	13	4	17	19	3	2	24	41	100	41	59
-1.00 V	28	8	4	6	10	43	3	2.5	48.5	58.5	94.5	17	83

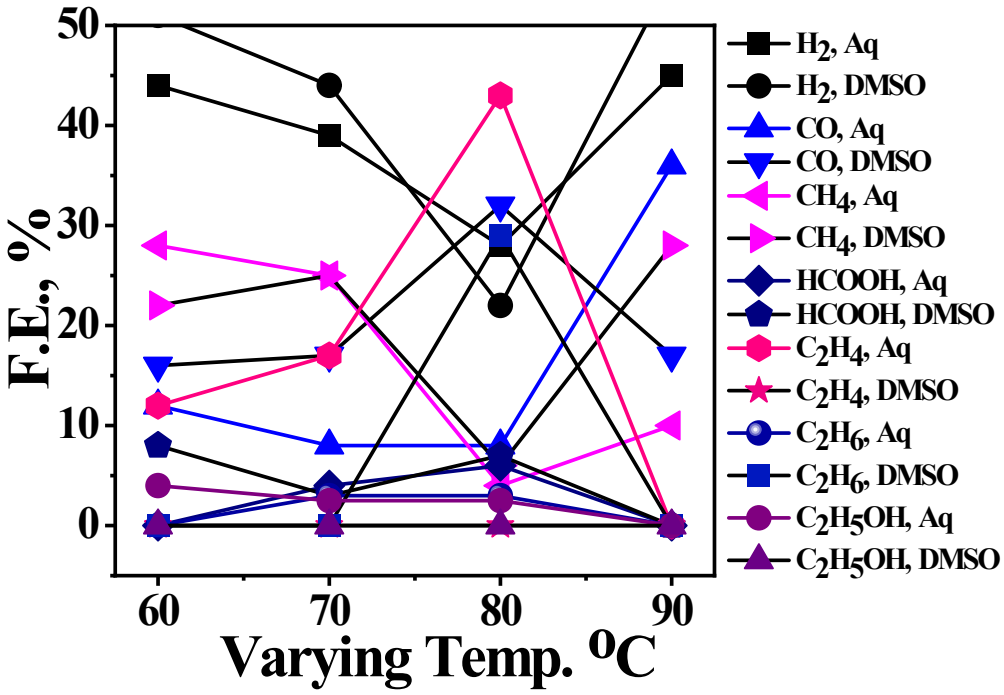

Figure SI-11. A comparison of the trend in variation of F.E. values for Cu-microstructure catalysts (prepared at varying electro-deposition temperatures) in DMSO and $KHCO_3$ aqueous medium.

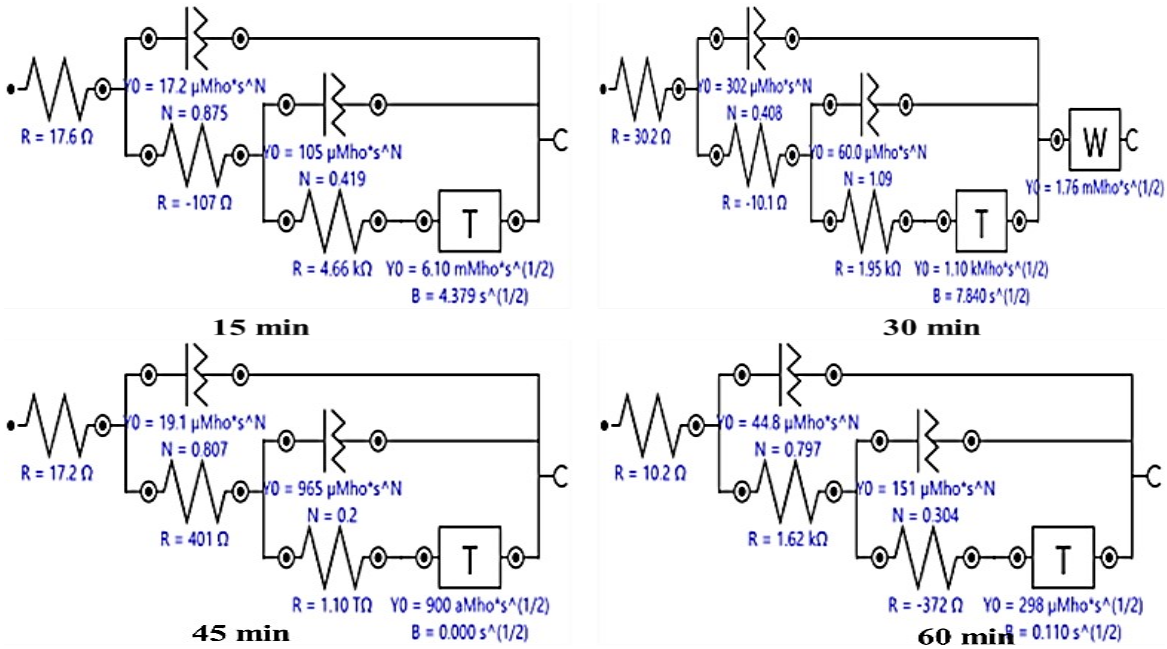

Figure SI-12: An equivalent circuits fitted to the Nyquist plots obtained on different Cu-micrstructures (prepared at varying electrodeposition times) in CO_2 saturated 0.2 M $KHCO_3$ at OCP.

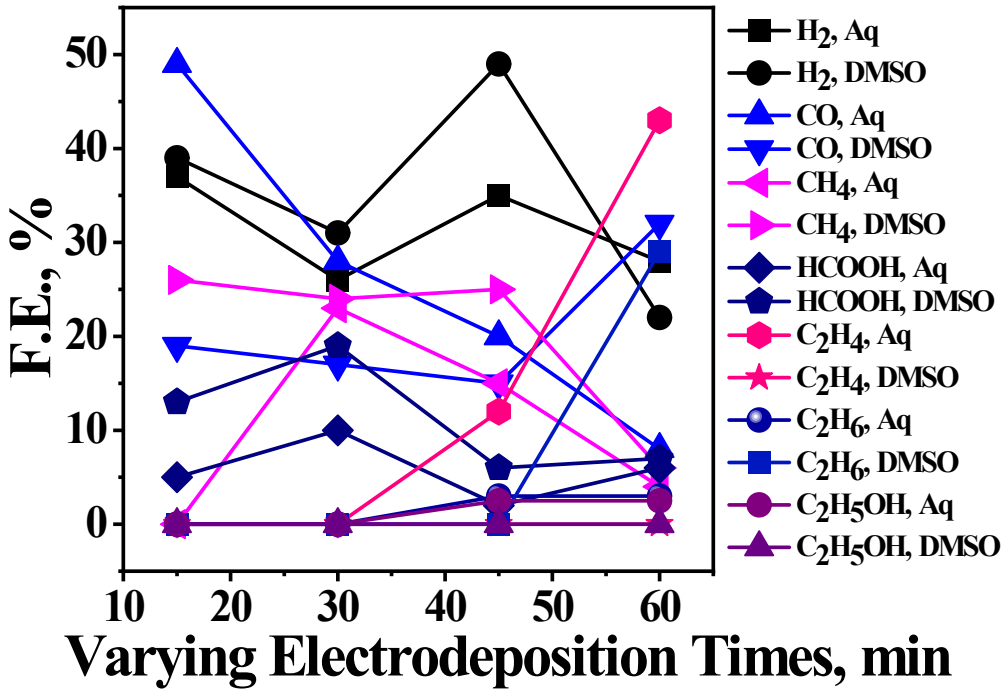

Figure SI-13. A comparison of the trend in variation of F.E. values for Cu-microstructure catalysts (prepared at varying electro-deposition times) in DMSO and $KHCO_3$ aqueous medium.

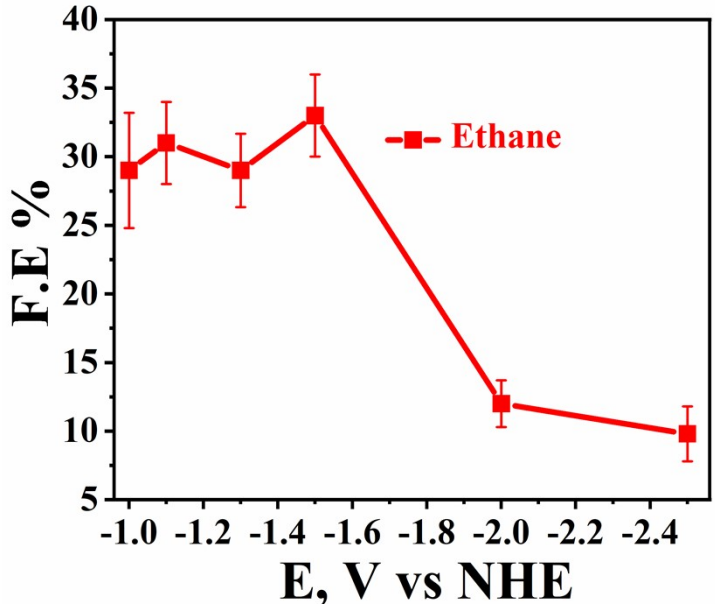

Figure SI-14: Change in ethane production with change in applied potential on optimised dendritic structure in DMSO electrolyte.

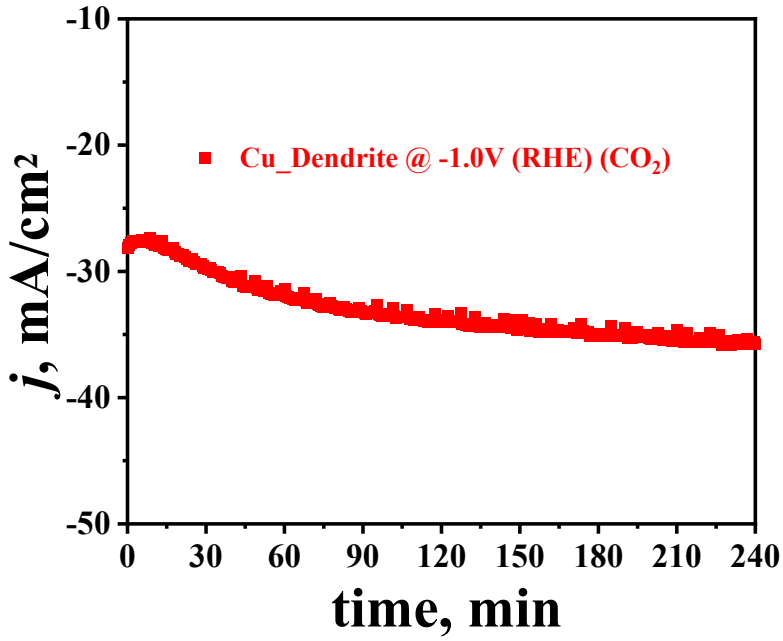

Figure SI-15: Stability of optimised copper dendrite (30V, 80 ^{0}C, 60 min and 100 mM AsH) in CO_2 for 3 hours.

Table SI-2: EIS fitting parameters of different samples at OCP as derived from the circuit fit.

Sample	R1(ohm)	Q1(Mho*s*N)	R2 (ohm)	Q2(Mho*s*N)	R3 (ohm)	T1(Mho*s*1/2)	W1(Mho*s*1/2)
25 mM	12.5	$119* 10^{-6}$	$-1.10* 10^{12}$	$6.10 * 10^{-6}$	--	--	$1.10*10^{12}$
75 mM	$603*10^{-3}$	$38.1*10^{-6}$	16	$5.65*10^{-6}$	$48.7*10^{3}$	--	--
7.5 V	9.84	$120*10^{-6}$	$1.71*10^{3}$	$179*10^{-6}$	-526	$365*10^{-6}$	--
15 V	-74.1	$781*10^{-6}$	94.6	$221*10^{-6}$	$-1.10*10^{12}$	$1.1*10^{3}$	$6.01*10^{-3}$
60 ^{0}C	6.18	$619*10^{-6}$	34.8	$92.9*10^{-6}$	-36.6	$46.8*10^{-3}$	$1.1*10^{-3}$
70 ^{0}C	10.8	$4.43*10^{-6}$	-68.0	$237*10^{-6}$	$1.47*10^{3}$	$96.7*10^{-6}$	--
90 ^{0}C	12.6	$1.15*10^{-6}$	-8.81	$969*10^{-6}$	$-1.1*10^{12}$	$4.75*10^{-3}$	--
15 min	17.6	$17.2*10^{-6}$	-107	$105*10^{-6}$	$4.66*10^{3}$	$6.10*10^{-3}$	--
30 min	30.2	$302*10^{-6}$	-10.1	$60*10^{-6}$	$1.95*10^{3}$	$1.10*10^{3}$	$1.76*10^{-3}$
45 min	17.2	$19.1*10^{-6}$	401	$965*10^{-6}$	$1.1*10^{12}$	$900*10^{-18}$	---
60 min	10.2	$44.8*10^{-6}$	$1.62*10^{3}$	$151*10^{-6}$	-372	$298*10^{-6}$	--

Table SI-3: EIS fitting parameters of optimised dendritic structure at different potentials as derived from the circuit fit.

Potential, V (RHE)	R1(ohm)	Q1(Mho*s*N)	R2 (ohm)	Q2(Mho*s*N)	R3 (ohm)	T1(Mho*s*1/2)	W1(Mho*s*1/2)
OCP	10.2	$44.8*10^{-6}$	$1.62*10^{3}$	$151*10^{-6}$	-372	$298*10^{-6}$	--
-0.324	11.0	$363*10^{-6}$	-2.93	$1.31*10^{-3}$	--	$1.57*10^{-3}$	$1.1*10^{12}$
-0.574	-4.37	$9.38*10^{-3}$	16.8	--	--	$264*10^{-3}$	$295*10^{-3}$
-0.724	9.83	$364*10^{-6}$	49.0	--	--	--	$205*10^{-3}$
-0.924	3.19	$180*10^{-6}$	18.2	$120*10^{-3}$	452	R4=5.74(ohm)	Q3=$814*10^{-6}$ (Mho*s*N)

Table SI-4: Morphology as a function of various synthetic parameters.

Sets of samples	Synthesis variable	Crystalline phase	Morphology observed
Set I	*Conc. Of Ascorbic acid*		
	25 mM (80 ^{0}C, 60 min, 30 V)	Cu (0), Cu_2O	Mixed (polygons and dendrites)
	75 mM (80 ^{0}C, 60 min, 30 V)	Cu (0)	Asymmetrical aggregates.
	100 mM (80 ^{0}C, 60 min, 30 V)	Cu (0)	Extensively branched dendrites.
Set II	*Applied voltage*		
	7.5 V (80^{0}C, 60 min, 100mM)	Cu (0)	Dendrites with few branches.
	15 V (80^{0}C, 60 min, 100mM)	Cu (0)	Coral reef structures with coupled dendrites.
	30 V (80^{0}C, 60 min, 100mM)	Cu (0)	Extensively branched dendrites.
Set III	*Temperature of reactor*		
	60 ºC (30V, 60 min, 100mM)	Cu (0), Cu_2O	Mixed (polygons and small dendrites)
	70 ºC (30V, 60 min, 100mM)	Cu (0), Cu_2O	Mixed (polygons and small dendrites)
	80 ºC (30V, 60 min, 100mM)	Cu (0)	Extensively branched dendrites.
	90 ºC (30V, 60 min, 100mM)	Cu (0), Cu_2O	Broken dendritic fragments and agglomerated structures.
Set IV	*Time of reaction*		
	10 min (30V, 80^{0}C, 100mM)	Cu (0)	Spheres
	15 min (30V, 80^{0}C, 100mM)	Cu (0), Cu_2O	Polygons
	30 min (30V, 80^{0}C, 100mM)	Cu (0), Cu_2O	Edge covered polygons
	45 min (30V, 80^{0}C, 100mM)	Cu (0), Cu_2O	Dendritic stems

	60 min (30V, 80^0C, 100mM)	Cu (0)	Extensively branched dendrites.

86